Research Article

Complex Electrochemical Behavior of Crystal Violet in Aqueous Solution in the Presence of Triton X-100

Iqbal Mahmud[1], Neamul H. Khansur[2,3], Md. Nizam Uddin[3], A.J.F. Samed[3], Md Abul Kalam[4,*], Md. Abu Bin Hasan Susan[5,*]

[1]Department of Electrical and Electronic Engineering, Eastern University, Dhaka 1205, Bangladesh
[2]Institute of Glass and Ceramics, Department of Materials Science and Engineering, Friedrich-Alexander-Universität Erlangen-Nürnberg, Martensstraße 5, 91058 Erlangen, Germany
[3]Department of Chemistry, Shahjalal University of Science and Technology, Sylhet 3114, Bangladesh
[4]Department of Natural Sciences, Texas A&M University-Texarkana, Texarkana, Texas 75503, USA
[5]Department of Chemistry, University of Dhaka, Dhaka-1000, Bangladesh
E-mail: md.kalam@tamut.edu; susan@du.ac.bd

Abstract: The electrochemical behavior of aqueous crystal violet in the presence of a nonionic surfactant, Triton X-100 (TX-100), was investigated using cyclic voltammetry. The cyclic voltammogram of crystal violet at a platinum electrode in an aqueous solution using 0.16 M NaCl as the supporting electrolyte was very sensitive to solution pH. In the pH range of 1.76 to 2.29, a well-defined voltammogram with one cathodic reduction peak and one anodic oxidation peak indicates unusual electrochemical reactions of crystal violet to yield the diquinoid of N,N,N',N'-tetramethyl benzidine (TMBOx) upon oxidation, which is reduced through a two-electron process to N,N,N',N'-tetramethyl benzidine (TMB). The cyclic voltammetric behavior of crystal violet in the presence of TX-100 surfactant, both below and above the critical micelle concentration, depends on the dissolved states of the surfactant. The electrochemical properties of crystal violet have been found to be diffusion controlled and dependent on TX-100 concentration. The electrochemical reaction is coupled with a preceding and a following chemical reaction and follows a CEC (chemical-electrochemical-chemical) mechanism. Interestingly, the unusual electrochemical reaction also occurs in the micellar system, and overall electrochemical behavior is dictated by the structure of crystal violet depending on the solution pH as well as the dissolved state of the surfactant. The findings of the present study may be useful to understand the host-guest chemistry of crystal violet and TX-100 at the molecular level.

Keywords: crystal violet, micelle, cyclic voltammetry, platinum electrode, pH

1. Introduction

Crystal violet, an organic dye, belongs to a class commonly known as triphenylmethane (TPM) dyes. The members of the TPM dyes, such as malachite green (MG), crystal violet [1], ethyl violet [2], and victoria blue B [3], are electrochemically active. Crystal violet and other TPM dyes have been widely used as antibacterial, antiseptic, and animal feeds, as well as in the industries such as textile, silk, and paper [4]. They are regarded as environmental hazards, and significant research efforts have been devoted to exploring their physiochemical properties aiming to find ways to minimize their environmental impacts [5, 6]. However, in recent years TPM dyes have drawn much attention due to their prospect for versatile uses other than traditional ones, including developing switchable molecular devices by controlling their electrochemical properties [7-10]. It is also worth investigating whether the unusual

electrochemical behavior is retained in organized media such as micellar systems and electrochemical responses correlate with the dissolved states of the surfactant in the presence of TPM dyes.

To gain further knowledge and find conditions to control the electrochemical properties of TMP dyes, researchers have been studying them under various electrolytic conditions. For instance, Perekotii *et al.* investigated the electrochemical behavior of crystal violet in potassium chloride, nitrate, and iodide supporting electrolytes using a glassy carbon electrode and found that crystal violet formed an electroactive complex with iodide adsorbed on the electrode while in a KI solution [1]. Galus and Adams reported that the electrochemical behavior of crystal violet in acidic aqueous media is complex. In the acidic solution, the ejection of the central carbon residue from the triphenylmethyl moiety followed by intramolecular coupling of the two phenyl fragments yields a diquinoid of N,N,N',N-tetramethyl benzidine (TMBOx) in the system, which proceeds via a two-electron redox process forms N,N,N',N-tetramethyl benzidine (TMB) [11, 12]. Hall *et al.* studied the electrochemical oxidation-reduction behavior of TMP dyes in liquid sulfur dioxide. The oxidation of the dyes in liquid sulfur dioxide was quite different from that observed in the acidic aqueous solution. Upon analysis of the voltammogram of crystal violet, they suggested that the redox couple generating the voltammogram on scanning from 0.50 to 1.50 V involved the carbonium ion and the formation of a free radical [13].

The interest in exploring the properties of electroactive compounds, including TPM dyes in surfactant-based organized media, has surged as their electrochemical behavior of redox-active probes has been found to be controllable by changing the concentration of surfactants [14, 15]. Saji *et al.* [16, 17] and Gokel and coworkers [18, 19] established the principle of electrochemical switching of redox-active amphiphiles. Saji *et al.* extensively studied the electrochemical properties of redox-active surfactants containing different electro-active groups aiming to form organic thin films on various electrode surfaces [16, 17]. They demonstrated that micelles formed by the surfactants could be dissociated into monomers by electrochemical oxidation, and this property could be used to form thin organic films. The investigation of the correlation of the electrochemical responses with the dissolved states of a nonionic ferrocenyl amphiphile was reported by Takeoka *et al.* [15, 20]. The authors showed that the characteristics of the cyclic voltammograms of the surfactant solutions depend on the dissolved states of the surfactants and the oxidation state of the redox-active moiety. Kozlecki *et al.* reported that adding an azo group to the hydrophobic tail of linear alkane sulfonates and alkane carboxylates promotes adsorption and micellization and improves surfactant solubility in water [21]. Susan *et al.* worked extensively on the electrochemical behavior of a series of redox-active nonionic surfactants containing anthraquinone and phenothiazine groups [22-25] and showed that surfactants respond interestingly to electrochemical changes and electrochemical behavior was found to be controllable by changing the concentration, structure, pH, and electrochemical potential of the redox-active surfactants. Various surfactants have also been tested in synthesizing compounds, such as electrolytic MnO_2. For instance, Minakshi and coworkers showed that electrolytic MnO_2 with an increased surface area could be prepared in the presence of TX-100 and Tween-20 [26]. Earlier studies on the electrochemical behavior of redox probes in electro-inactive surfactants have been reviewed by Rusling [27]. Redox-active ferrocene, anthraquinone, and phenothiazine have been used by Susan and coworkers as probes to study the electrochemical behavior in aqueous solutions in the presence of different surfactants to reveal that the concept of electrochemical switching is also applicable for redox probes solubilized in organized media of electro-inactive surfactants [28-32]. Yeh also estimated the diffusion coefficient of the micelles of an electro-inactive surfactant, Tween 20, using a probe molecule, ferrocene, which is solubilized in the micelles [33]. Recently, Rahman *et al.* [34] investigated the electrochemical behavior of malachite green (MG) oxalate in the aqueous solution in the presence of a cationic surfactant, cetyltrimethylammonium bromide (CTAB), and an anionic surfactant, sodium dodecyl sulfate (SDS) at a glassy carbon electrode using cyclic voltammetry. The authors have reported significant interaction of MG with different surfactants. Their investigation also revealed that the electrochemical oxidation of MG is an irreversible diffusion-controlled process under ambient conditions. Despite numerous studies on electrochemically switchable systems, the electrochemical study of TPM dyes in the presence of a surfactant system is still in the rudimentary stage, and in particular, a study of crystal violet is yet to be reported. With a view to understanding the electrochemical behavior of crystal violet in an aqueous solution in the presence of TX-100, we aimed at a systematic study of the cyclic voltammetric behavior in a wide range of TX-100 concentrations. The ultimate goal is to correlate the unusual electrochemical reaction of crystal violet with the dissolved states of the surfactants.

2. Experiments

Crystal violet and sodium chloride (NaCl) were purchased from BDH and used as received. Polyoxyethylene ter-octylphenyl ether, $[(H_3C)_3CH_2C(CH_3)_2C_6H_4-(OCH_2CH_2)_{9.5}-OH]$, known as TX-100, was obtained from BDH and used without further purification. All the stock solutions were prepared with Puric-S grade deionized water (Specific resistance = 2.00 MΩ cm, Organo Co., Tokyo). While investigating the electrochemistry of crystal violet in the presence of TX-100, the crystal violet concentration was maintained at 8.80×10^{-8} M; otherwise, it was kept constant at 1.00×10^{-6} M for other experiments. Glassware used for preparing micellar solutions of TX-100 was first washed with NaOH solution and then with a large excess of deionized water. TX-100 solutions of varying concentrations were prepared using the stock solution by proper dilution.

A pH meter (HM-26S, TOA electronics Ltd., Japan) was used to measure the pH of the solutions. The solutions were bubbled with nitrogen to avoid any contribution in the measured pH from CO_2 dissolved from the atmosphere. For the cyclic voltammetric measurements, a computer-controlled electrochemical analyzer (Model HQ 2040 by Advanced Analytics, USA) was employed. A single-compartment three-electrode cell was used for electrochemical measurements. The three electrodes used in the cell are as follows: a platinum electrode (BAS) with a geometric area of 0.021 cm² as a working electrode, an Ag/AgCl as the reference electrode, and a Pt-wire as a counter electrode. The working electrode surface was mirror-polished and cleaned by polishing with 0.05 μm alumina (Buehler) at each measurement. Before the electrochemical experiments, the solutions were purged with N_2, and the inert atmosphere was kept during the experiments. The measurements were carried out using a 0.16 M NaCl aqueous solution as the supporting electrolyte. The potential sweep rate (v) was between 10 and 500 mVs⁻¹. All the measurements were conducted at 25.0 °C.

3. Results and Discussion

Electrochemistry of aqueous crystal violet in the absence of TX-100 and its pH dependence: Cyclic voltammetric behavior of crystal violet was investigated at different pH values in the range from 1.54 to 11.75 in the presence of NaCl (0.16 M) as the supporting electrolyte. The profiles of five representative experimental voltammograms are presented in Fig. 1.
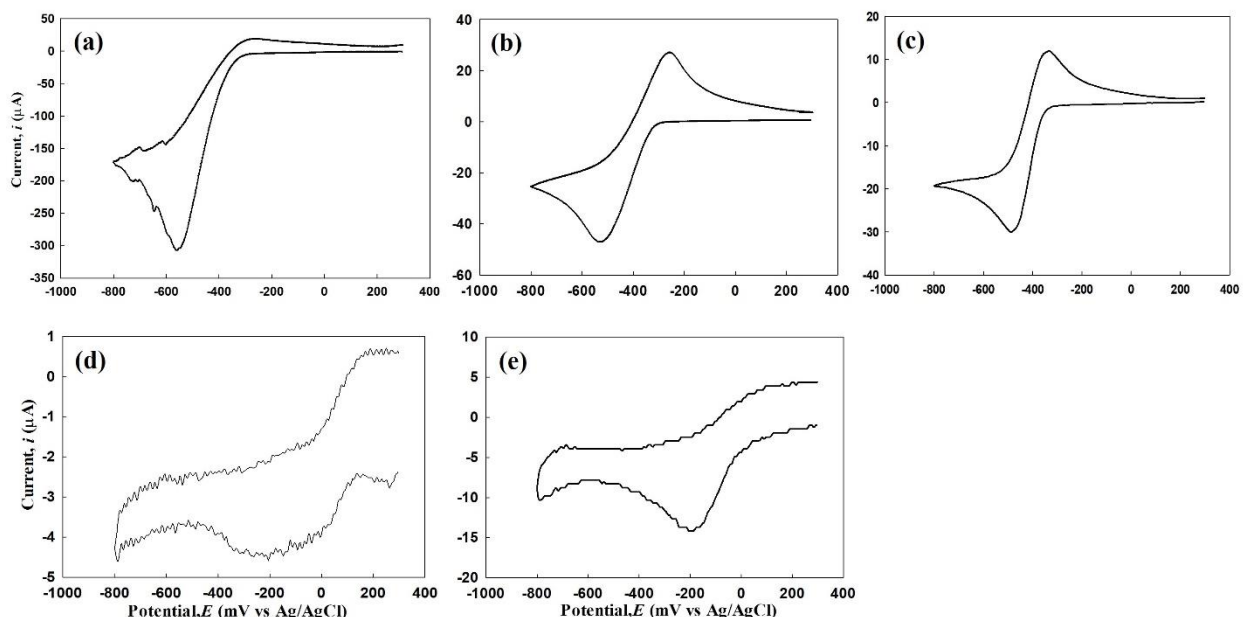
Fig. 1: Cyclic voltammograms of 1.00×10^{-6} M of crystal violet in 0.160 M NaCl acidic aqueous solution at pH= (a) 1.54 (b) 1.86 (c) 2.29 (d) 4.96 and (e) 11.75. The potential was scanned from 300 to -800 mV, followed by a reverse scan from -800 to 300 mV (v =10 mVs⁻¹).

As shown in Fig. 1(a-e), the electrochemical behavior of aqueous crystal violet depends on the pH of the solution medium. The pH range of 1.76 to 2.29 provides crystal violet with the condition to produce a well-shaped voltammogram with one cathodic and one anodic peak (Fig. 1(b) and (c)). At a very low pH (<1.76), crystal violet loses reversibility, and no well-defined anodic peak could be observed (Fig. 1(a)). At the pH of 4.96 (pH of the aqueous solution of crystal violet with no added H^+), no significant current signals could be detected (Fig. 1(d)). On the other hand, at high pH (e.g., pH=11.75), the cyclic voltammogram attains a new shape indicating the possibility of a different electrochemical reaction (Fig. 1(e)). The observed characteristics of the voltammograms are supported by the published literature [11, 12]. According to the literature, in solution, crystal violet could exist in different forms depending on the pH of the medium (Scheme 1)

Neutral to Acidic

I	II	III
(Neutral pH)	(Low pH)	(Very low pH)

Neutral to Alkaline

IV	V	VI
(Neutral pH)	(High pH)	(Very high pH)
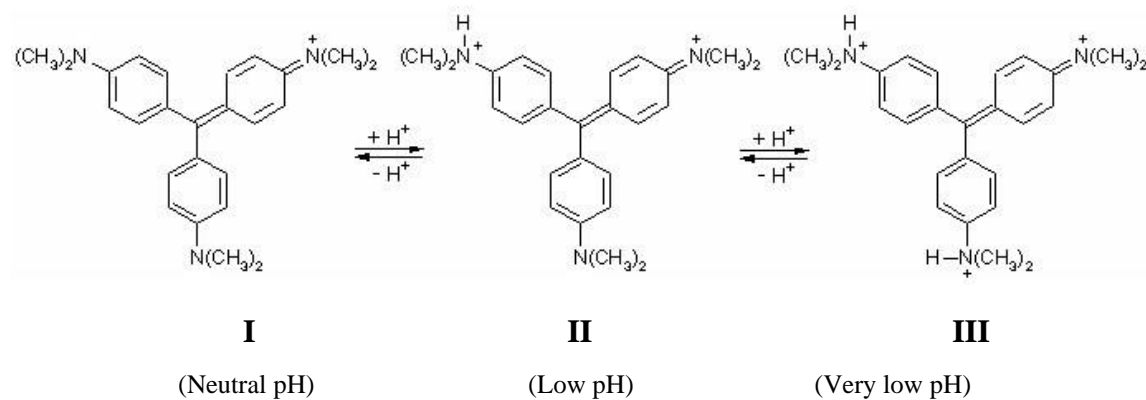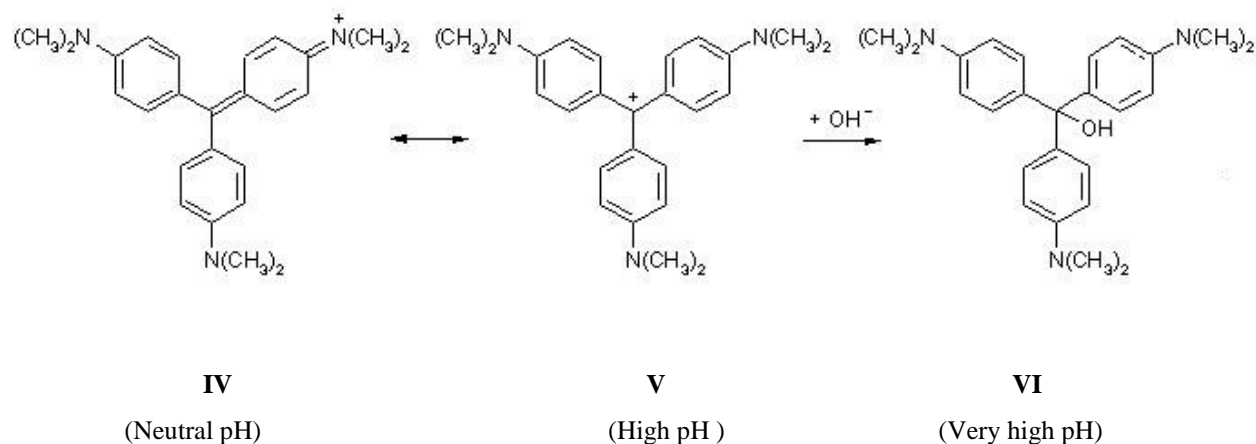
Scheme 1: Probable structures of crystal violet and their interconversion with the change in pH of the aqueous medium [11].
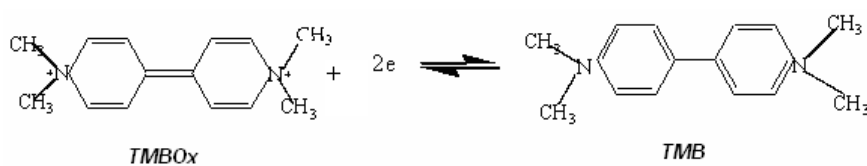
Scheme 2: Redox reaction of TMBOx and TMB. Structure II (Scheme I) could break down to give rise to TMBOx.

As presented in Scheme 1, at very low pH (e.g., pH ~ 1.54), crystal violet exists in a form with three positive charges on three nitrogens (structure **III**) and gives rise to the voltammogram described in Fig. 1(a). Similarly, at pH 4.96, structure **I** produces the voltammogram shown in box Fig. 1(d). Around pH 2.29, crystal violet exists in the stable protonated dication form (Structure **II**). As reported in the literature, triphenylmethane dyes in acidic aqueous buffered solution show unusual electrochemical reactions. The ejection of the central carbon residue from the triphenylmethyl moiety followed by intramolecular coupling of the two phenyl fragments leads to the formation of compounds of TMBOx. Cyclic voltammetry in acidic buffers revealed that the hydrated and protonated form of the dye upon oxidation results in the intramolecular coupling reaction to yield TMBOX. This dication could form TMBOx, which in turn could participate in a two-electron transfer process, depicted in Scheme 2, to form TMB [11]. Hence, we predict that the cyclic voltammogram shown in Fig. 1(b) corresponds to the electrochemical reaction of the redox couple, TMBOx/TMB. To confirm, lead peroxide in sulfuric acid was used to oxidize crystal violet, and the product was isolated and subjected to cyclic voltammetric measurements in solution. The cyclic voltammogram (Figure not shown) agreed well with the TMB-TMBOx redox system formed by the electrochemical method under applied potential. This is in excellent agreement with our previous observations on another TPM dye, Malachite green [34]. However, the newly established electrochemical process may give rise to a complex voltammogram with multiple anodic peaks if the electrode is not cleaned after each cycle and the voltammogram is recorded at a different potential range and scan direction [11].

At high pH (basic range), the voltammogram has a different shape, as the formation of TMBOx is not possible in the basic solution. Rather the carbocationic form (Scheme 1) of crystal violet undergoes an electrochemical reduction reaction to form leucocrystal violet, followed by its oxidation to crystal violet, thereby producing the voltammogram shown in Fig. 1(d).
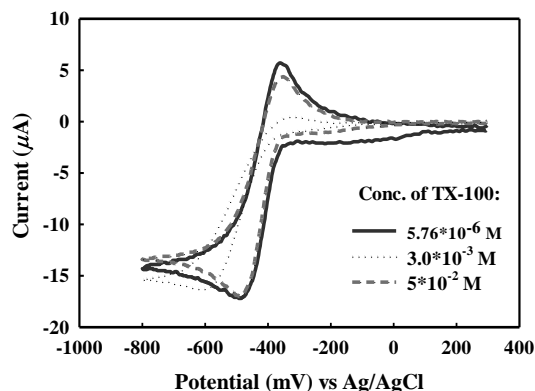
Fig. 2: Cyclic voltammograms of 8.80×10^{-8} M crystal violet in various concentrations of TX-100 at a scan rate of 10 mVs^{-1} (0.160 M NaCl aqueous solution is used as a supporting electrolyte).

Electrochemistry of Crystal Violet in the presence of TX-100 in Aqueous Solution: The cyclic voltammograms of crystal violet were acquired in the presence of TX-100 at pH 2.16 and well-defined voltammograms could be obtained at this pH. In addition, the concentration of crystal violet was chosen 8.80×10^{-8} M (instead of 1.00×10^{-6} M used for the analysis of the pH dependence) for this experiment to minimize the effect of crystal violet on the critical

micelle concentration (CMC) of TX-100 (8.75×10^{-4} M at 25 °C). Generally, adding electrolytes or electro-active substances (e.g., crystal violet) lowers the CMC value [24]. Therefore, the CMC of aqueous TX-100 in the presence of NaCl and crystal violet is likely to be slightly lower than 8.75×10^{-4} M at 25 °C. To evaluate the effect of TX-100 on the electrochemical behavior of crystal violet, the voltammograms of crystal violet were recorded at a scan rate of 10 mVs^{-1} at a wide range of TX-100 concentrations in the range of 0.00288- 50.0 mM. Nevertheless, for clarity, the representative voltammograms recorded at three TX-100 concentrations (0.0576, 3.00, and 50.0 mM) are shown in Fig. 2. It is noticeable that the general shape characteristics of the voltammograms obtained at various concentrations of TX-100 are similar to those produced in the absence of TX-100 at pH 2.29. The peak potentials also have a similar pattern and remain virtually constant over the experimental range of TX-100 concentrations (figure not shown). However, the variation of the peak currents with TX-100 concentration implies that the electrochemical responses depend on the concentration of TX-100.
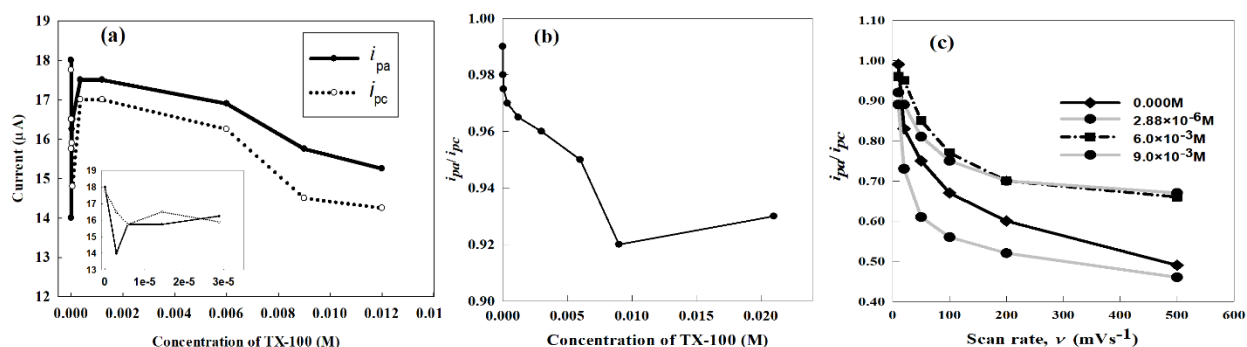
Fig. 3: Peak current profile of 8.80×10^{-8} M crystal violet in various TX-100 concentrations; (a) Anodic and cathodic current profiles as a function of TX-100 concentration ($v=10$ mVs^{-1}), (b) The anodic and cathodic current ratio (i_{pa}/i_{pc}) as a function of TX-100 concentration ($v=10$ mVs^{-1}), (c) The anodic and cathodic current ratio (i_{pa}/i_{pc}) as a function of scan rate.

Fig. 3(a) depicts the dependence of the anodic peak current (i_{pa}) and the cathodic peak current (i_{pc}) with the concentration of TX-100. It is evident that both i_{pa} and i_{pc} show almost similar behavior with the change in TX-100 concentration. As the concentration of TX-100 increases, initially, the cathodic peak current decreases slightly, and when it reaches the CMC, it decreases sharply. Below the CMC, surfactant species exist as free monomers; therefore, crystal violet diffuses freely to the electrode interface. This gives rise to a relatively high peak current at low surfactant concentrations because of the presence of reducible TMBOx at this pH under the applied potential. At the CMC, surfactant species aggregate to form thermodynamically stable oriented aggregates of colloidal dimension, *i.e.*, micelles. Crystal violet is easily solubilized inside the core of the micelle. Consequently, the diffusion of crystal violet to the electrode interface is slower, causing the reduction in cathodic peak current. Similarly, as the concentration of TX-100 reaches just above the CMC, the cathodic peak current decreases drastically since practically all the electroactive species have been trapped inside the core of the micelles.

Fig. 3(b) illustrates the change in the ratio of anodic peak current to cathodic peak current (i_{pa}/i_{pc}) with TX-100 concentration. The i_{pa}/i_{pc} shows an abrupt decrease with increasing concentration of TX-100 at the beginning; then, a gradual decrease occurs up to the CMC. Above and beyond the CMC, i_{pa}/i_{pc} increases slightly as TX-100 concentration is increased. It is apparent that the i_{pa}/i_{pc} has a value less than 1 irrespective of the presence of TX-100, suggesting that the electrochemical reaction might be coupled with a following chemical process. As the ratio decreases with the increase of TX-100 concentration, the kinetics of the following processes are influenced by the presence of TX-100.

To determine whether the electrochemical reaction is also coupled with a preceding chemical reaction, i_{pa}/i_{pc} is plotted as a function of the scan rate (Fig. 3(c)). As depicted in Fig. 3(c), the i_{pa}/i_{pc} decreases with the scan rate, but the values of the i_{pa}/i_{pc} in the presence of TX-100 are always higher than that in the absence of TX-100. The decrease in the i_{pa}/i_{pc} with the scan rate coincides with the behavior of a reversible electrochemical reaction coupled with a preceding chemical reaction, which resembles the behavior in the absence of TX-100. In the present case, the most probable preceding reaction is the formation of TMBOx from crystal violet and the protonation of the carbocationic dye to form the protonated form at low pH, even in the presence of TX-100. The higher values of the i_{pa}/i_{pc} in the

presence of TX-100 at any scan rate further indicate that the rate of the following chemical process in the presence of the TX-100 solution is slower compared to that in the absence of TX-100.

The cathodic peak current for crystal violet was further analyzed to find whether the change in TX-100 concentration causes a change in adsorption at the electrode surface or diffusion to dominate the overall electrochemical process. Fig. 4(a-b) describes the scan rate dependence of the i_{pc} and the cathodic peak potential (E_{pc}) for different TX-100 concentrations. It shows that the E_{pc} is shifting negatively in response to the increase in the scan rate, suggesting that the system might be a *quasi-reversible* one (Fig. 4(a)).

(a)   **(b)**
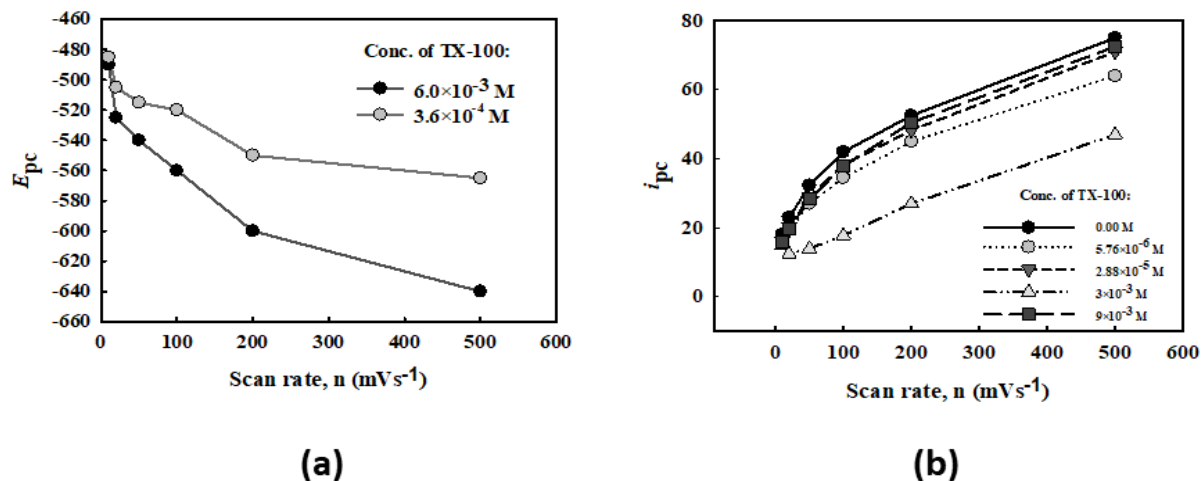
Fig. 4: A plot of (a) cathodic peak potential and (b) cathodic peak current (i_{pc}) versus scan rate at different TX-100 concentrations for an aqueous solution of 8.80×10^{-8} M crystal violet in 0.160 M NaCl.

It is also evident from Fig. 4(b) that i_{pc} increases nonlinearly with the scan rate. The nonlinear increase of i_{pc} further supports the notion of a *quasi-reversible* process. In addition, the non-linearity of the i_{pc} vs. v plots, as shown in Fig. 4(b), confirms that rather than adsorption, some other processes are dominating the electrochemical process.

For further evaluation - whether the electrochemical behavior of crystal violet in TX-100 is adsorption- or diffusion-controlled, the peak current data was further analyzed. The value of the slope of the $\log i_{pc}$ vs. $\log v$ plots at all TX-100 concentrations is below 0.5, indicating that the process is a diffusion-controlled one [35]. Since the value of the slope is slightly lower than 0.5, the reaction is likely to be preceded by a chemical reaction. In the present case, it is the formation of TMBOx from crystal violet and the protonation of the carbocationic dye to form the protonated form even in the presence of TX-100.

In the case of a freely diffusing redox species, the Randles-Sevcik equation describes the cathodic peak current of an electrochemically reversible process at 25°C as

$$i_{pc} = (2.69 \times 10^5) \, n^{3/2} \, A D_{app} \, v^{1/2} \, C \tag{1}$$

where i_{pc} is the cathodic peak current in amperes, n is the number of electrons taking part in the electrochemical reaction, A is the geometric area of the electrode surface m², D_{app} is the apparent diffusion coefficient of electroactive species in m²s⁻¹, v is the potential scan rate in Vs⁻¹ and C is the concentration (mol m⁻³) of the reactive species in the bulk of the solution.

The apparent diffusion coefficient, D_{app}, of crystal violet has been approximated using equation 1, and the values at different concentrations of TX-100 are presented in Fig. 5.
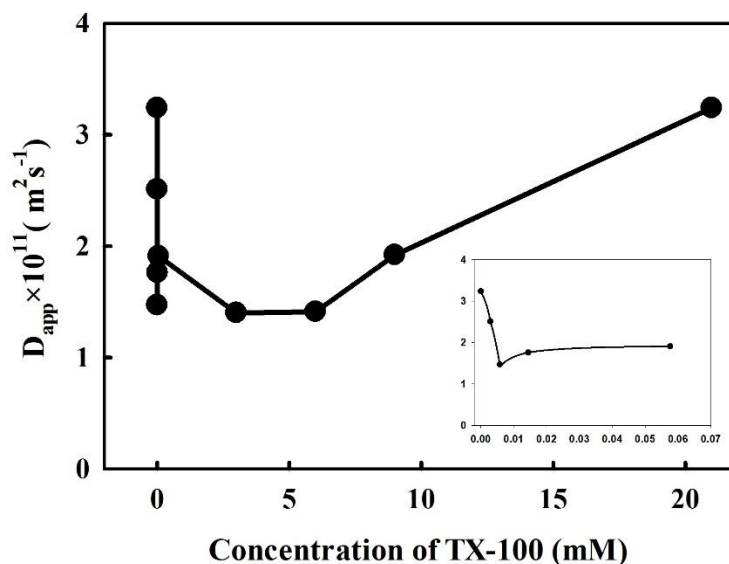
Fig. 5: Dependence of the apparent diffusion coefficient of crystal violet (8.80×10^{-8} M) on the concentrations of TX-100.

The D_{app} value, exhibited in Fig. 5, decreases with increasing TX-100 concentration, passes through a minimum, and then increases. At TX-100 concentrations abovethe CMC, it is believed that crystal violet is solubilized inside the core of micelles, and diffusion of crystal violet or TMBOx to the electrode interface is lowered. At higher concentrations, the number of micellar TX-100 aggregates increases, which reduces the concentration of TMBOx in the micellar pseudo phase. As a result, the distance between the electrode surface and TMBOx inside the core of the micelle is too long to undergo the electron-transfer reaction. It is, therefore, reasonable to consider that the electrochemical reaction occurs in the monomeric form, and the diffusivity increases above the CMC.

4. Conclusion

The electrochemical properties of crystal violet in the aqueous medium are pH-dependent, producing well-defined cyclic voltammograms in the pH range of 1.76 to 2.29. The presence of Triton X-100 does not influence the shape of the voltammograms in the same range. The electrochemical reaction at a platinum electrode in an aqueous solution has been complex and unusual, and it is retained even in the presence of Triton X-100, both below and above critical micelle concentration. However, the electrochemical behavior of crystal violet depends on the concentration of Triton X-100 and the dissolved states of the surfactant. The peak current, peak potential, and diffusivity changed depending on the concentration of the surfactants since a change in concentration caused a transition from monomeric surfactant to self-assembled micellar species. The voltammograms recorded around pH 2.0 are attributed largely to diquinoid of N,N,N',N'- tetramethyl benzidine (TMBOx)/ N,N,N',N'-tetramethyl benzidine (TMB) redox couple, and the redox process appears to be diffusion controlled. The data analysis of peak currents suggests that the electron transfer between TMBOx and TMB might be coupled with the preceding chemical reaction and a following chemical process.

Conflict of Interests

The authors declare no conflicts of interest.

Acknowledgments

References

[1] Perekotii, V.V.; Temerdashev, Z.A.; Tsyupko, T.G.; Palenaya, E.A. Electrochemical Behavior of Crystal Violet on Glassy Carbon Electrodes. *J. Anal. Chem.* **2002**, *57*, 448–451, https://doi.org/10.1023/a:1015421927771.

[2] Song, J.-P.; Guo, Y.-J.; Shuang, S.-M.; Dong, C. Study on the inclusion interaction of ethyl violet with cyclodextrins by MWNTs/Nafion modified glassy carbon electrode. *J. Incl. Phenom. Macrocycl. Chem.* **2010**, *68*, 467–473, https://doi.org/10.1007/s10847-010-9811-7.

[3] Xu, B.; Jiao, K.; Sun, W.; Zhang X. Recognition and determination of DNA using victoria blue b as electrochemical probe. Int. J. Electrochem. Sci. **2007,** 2, 406–417. https://oa.mg/work/3184054570.

[4] Ali, S.A.; Ahmed, G.; Hamiz-Ul-Fawwad, S.; Waqar, S.A.; Saleem, A. Gentian violet – A blessing in disguise for the developing world. *Burns* **2013**, *39*, 1326–1327, https://doi.org/10.1016/j.burns.2013.02.004.

[5] Pillai, I.M.S.; Gupta, A.K.; Sahoo, C. Electrochemical Oxidation of Crystal Violet Dye (Basic Violet 3) using Lead Oxide Electrodes. **2011**, https://doi.org/10.2316/p.2011.736-047.

[6] Petcu, A.R.; Rogozea, E.A.; Lazar, C.A.; Olteanu, N.L.; Meghea, A.; Mihaly, M. Specific interactions within micelle microenvironment in different charged dye/surfactant systems. *Arab. J. Chem.* **2016**, *9*, 9–17, https://doi.org/10.1016/j.arabjc.2015.09.009.

[7] Ariga, K.; Kunitake, T. *Supramolecular Chemistry: Fundamentals and Applications*, 1st ed.; Springer: Berlin, Germany, 2006; pp. 1–208, https://doi.org/10.1007/b137036.

[8] Selvakumar, P.M. The Art of Converting Molecules into Machines: Supramolecular Chemistry. *MOJ Bioorganic Org. Chem.* **2017**, *1*, 1–3, https://doi.org/10.15406/mojboc.2017.01.00021.

[9] Toma, H.E. Supramolecular nanotechnology: from molecules to devices. *Curr. Sci.* **2008**, 95, 1202–1025. https://www.jstor.org/stable/24103233.

[10] Ge, W.; Chen, Y.; Fan, Y.; Zhu, Y.; Liu, H.; Song, L.; Liu, Z.; Lian, C.; Jiang, H.; Li, C. Dynamically Formed Surfactant Assembly at the Electrified Electrode–Electrolyte Interface Boosting CO_2 Electroreduction. *J. Am. Chem. Soc.* **2022**, *144*, 6613–6622, https://doi.org/10.1021/jacs.2c02486.

[11] Galus, Z.; Adams, R.N. The Anodic Oxidation of Triphenylmethane Dyes. *J. Am. Chem. Soc.* **1962**, *84*, 3207–3208, https://doi.org/10.1021/ja00875a049.

[12] Galus, Z.; Adams, R.N. The Anodic Oxidation of Triphenylmethane Dyes. *J. Am. Chem. Soc.* **1964**, *86*, 1666–1671, https://doi.org/10.1021/ja01063a003.

[13] Hall, D.; Sakuma, M.; Elving, P. Voltammetric oxidation of triphenylmethane dyes at platinum in liquid sulphur dioxide. *Electrochimica Acta* **1966**, *11*, 337–350, https://doi.org/10.1016/0013-4686(66)87044-5.

[14] Saji, T.; Hoshino, K.; Aoyagui, S. Reversible formation and disruption of micelles by control of the redox state of the head group. *J. Am. Chem. Soc.* **1985**, *107*, 6865–6868, https://doi.org/10.1021/ja00310a020.

[15] Takeoka, Y.; Aoki, T.; Sanui, K.; Ogata, N.; Watanabe, M. Electrochemical Studies of a Redox-Active Surfactant. Correlation between Electrochemical Responses and Dissolved States. *Langmuir* **1996**, *12*, 487–493, https://doi.org/10.1021/la9501290.

[16] Saji, T.; Ebata, K.; Sugawara, K.; Liu, S.; Kobayashi, K. Electroless Plating of Organic Thin Films by Reduction of Nonionic Surfactants Containing an Azobenzene Group. *J. Am. Chem. Soc.* **1994**, *116*, 6053–6054, https://doi.org/10.1021/ja00092a100.

[17] Saji, T.; Hoshino, K.; Ishii, Y.; Goto, M. Formation of organic thin films by electrolysis of surfactants with the ferrocenyl moiety. *J. Am. Chem. Soc.* **1991**, *113*, 450–456, https://doi.org/10.1021/ja00002a011.

[18] Munoz, S.; Gokel, G.W. Redox-switched vesicle formation from two novel, structurally distinct metalloamphiphiles. *J. Am. Chem. Soc.* **1993**, *115*, 4899–4900, https://doi.org/10.1021/ja00064a064.

[19] Wang, K.; Muñoz, S.; Zhang, L.; Castro, R.; Kaifer, A.E.; Gokel, G.W. Organometallic Amphiphiles: Oxidized Ferrocene as Headgroup for Redox-Switched Bilayer and Monolayer Membranes. *J. Am. Chem. Soc.* **1996**, *118*, 6707–6715, https://doi.org/10.1021/ja953177f.

[20] Takeoka, Y.; Aoki, T.; Sanui, K.; Ogata, N.; Yokoyama, M.; Okano, T.; Sakurai, Y.; Watanabe, M. Electrochemical control of drug release from redox-active micelles. *J. Control. Release* **1995**, *33*, 79–87, https://doi.org/10.1016/0168-3659(94)00078-9.

[21] Koźlecki, T.; Sokołowski, A.; Wilk, K.A. Surface Activity and Micelle Formation of Anionic Azobenzene-Linked Surfactants. *Langmuir* **1997**, *13*, 6889–6895, https://doi.org/10.1021/la970035l.

[22] Susan, A.B.H.; Begum, M.; Takeoka, Y.; Watanabe, M. Study of the Correlation of the Cyclic Voltammetric Responses of a Nonionic Surfactant Containing an Anthraquinone Group with the Dissolved States. *Langmuir* **2000**, *16*, 3509–3516, https://doi.org/10.1021/la991033z.

[23] Susan, M.B.H.; Begum, M.; Takeoka, Y.; Watanabe, M. Effect of pH and the extent of micellization on the redox behavior of non-ionic surfactants containing an anthraquinone group. *J. Electroanal. Chem.* **2000**, *481*, 192–199, https://doi.org/10.1016/s0022-0728(99)00493-3.

[24] Susan, A.; Ishibashi, A.; Takeoka, Y.; Watanabe, M. Surface activity and redox behavior of a non-ionic surfactant containing a phenothiazine group. *Colloids Surfaces B: Biointerfaces* **2004**, *38*, 167–173, https://doi.org/10.1016/j.colsurfb.2004.01.016.

[25] Susan, M.A.B.H.; Tani, K.; Watanabe, M. Surface activity and redox behavior of nonionic surfactants containing an anthraquinone group as the redox-active site. *Colloid Polym. Sci.* **1999**, *277*, 1125–1133, https://doi.org/10.1007/s003960050501.

[26] Biswal, A.; Tripathy, B.C.; Subbaiah, T.; Meyrick, D.; Ionescu, M.; Minakshi, M. Effect of Non-ionic Surfactants and Its Role in K Intercalation in Electrolytic Manganese Dioxide. *Met. Mater. Trans. E* **2014**, *1*, 226–238, https://doi.org/10.1007/s40553-014-0022-9.

[27] Rusling, J.F. Electroanalytical Chemistry. New York, USA; Marcel Dekker: 1994.

[28] Haque, M.A.; Rahman, M.M.; Susan, M.A.B.H. Aqueous Electrochemistry of Anthraquinone and Its Correlation with the Dissolved States of a Cationic Surfactant. *J. Solut. Chem.* **2011**, *40*, 861–875, https://doi.org/10.1007/s10953-011-9690-6.

[29] Mahmud, I.; Samed, A.; Haque, A.; Susan, A.B.H. Electrochemical behavior of anthraquinone in aqueous solution in presence of a non-ionic surfactant. *J. Saudi Chem. Soc.* **2011**, *15*, 203–208, https://doi.org/10.1016/j.jscs.2010.08.006.

[30] Haque, M.A.; Rahman, M.M.; Susan, M.A.B.H. Electrochemical Behavior of Anthraquinone in Reverse Micelles and Microemulsions of Cetyltrimethylammonium Bromide. *J. Solut. Chem.* **2012**, *41*, 447–457, https://doi.org/10.1007/s10953-012-9810-y.

[31] Keya, J.J.; Islam, M.; Rahman, M.M.; Mollah, M.Y.A.; Susan, A.B.H. Effect of a water structure modifier on the aqueous electrochemistry of supramolecular systems: Redox-active versus conventional surfactants. *J. Electroanal. Chem.* **2014**, *712*, 161–166, https://doi.org/10.1016/j.jelechem.2013.11.019.

[32] Roy, C.K.; Saha, S.; Susan, A.B.H. Control Over Diffusion of Ionic Ferrocene Species in Aqueous Solution Using Surfactant Based Organized Media. *J. Electrochem. Soc.* **2020**, *167*, 116512, https://doi.org/10.1149/1945-7111/aba400.

[33] Yeh, P.; Kuwana, T. The Electrochemistry of Micelle-Solubilized Ferrocene. *J. Electrochem. Soc.* **1976**, *123*, 1334–1339, https://doi.org/10.1149/1.2133071.

[34] Rahman, M.M.; Mollah, M.Y.A.; Susan, A.B.H. Electrochemical Behavior of Malachite Green in Aqueous Solutions of Ionic Surfactants. *ISRN Electrochem.* **2013**, *2013*, 1–10, https://doi.org/10.1155/2013/839498.

[35] Bard, A.J.; Faulkner, L.R.; White, H.S. Electrochemical Methods: Fundamentals and Applications, 3rd ed. Wiley; 2022.